JOURNAL OF SOLID STATE CHEMISTRY 98, 59–70 (1992)

Electronic Structure and Properties of Anionic Mixed Valence and Layered $CrTe_3$: The Question of Extended Tellurium Bonding in Transition Metal Tellurides

E. CANADELL,* S. JOBIC,† R. BREC,† AND J. ROUXEL†

Laboratoire de Chimie Théorique, Université de Paris Sud, 91405, Orsay, France; and †Laboratoire de Chimie des Solides, Institut des Matériaux de Nantes, 2 rue de la Houssinière, 44072, Nantes Cédex 03, France

Received June 24, 1991; in revised form October 25, 1991

$CrTe_3$ is a layered material whose tellurium sublattice contains Te, Te_2, and Te_3 entities. Our magnetic susceptibility measurements are consistent with a +3 oxidation state for Cr. This indicates three different oxidation states for the tellurium atoms, i.e., Te^{2-}, Te_2^{2-}, and Te_3^{2-}. Conductivity measurements show this material to be a semiconductor with an activation energy of 0.35 eV. Our tight-binding band structure calculations indicate that it is a Mott–Hubbard semiconductor rather than a regular one. A study of the Te···Te overlap populations suggests that $CrTe_3$ is a new transition metal telluride with a polymerized tellurium network. Analysis of this additional bonding within the tellurium sublattice in this phase and in related tellurides leads to a classification of the transition metal ditellurides taking into account both dimensionality and degree of polymerization.

I. Introduction

Contrary to tellurides, sulfides and selenides have been extensively studied for their chemical and physical properties. Special attention has been devoted to binary compounds, in particular the low-dimensional ones, because of their strong anisotropy and their numerous potential applications. Because of the loss in its bonding directionality, tellurium does not lead so frequently to low-dimensional compounds. It is also a very heavy and absorbing element that renders crystal structure determination more difficult and from which compounds seem to be more difficult to obtain in the pure state because of synthesis equilibrium problems. This may explain why the chemistry and physics of tellurides are not so much developed and well known as those of parent sulfides and selenides. With better analytical and synthesis tools, along with efficient structure determination programs, more syntheses and studies on tellurides appear in the literature. One article reported recently the synthesis and structure determination of a new layered chromium telluride $CrTe_3$ (*1*). Recent studies on several families of ditellurides of transition metals (*2–4*) have shown that it was necessary, in most of these phases, to add polymeric modifications to the well known CdI_2-like and pyrite-like structure types in order to take into account the multiple bondings between tellurium anions. To respond to the cation oxidation state, tellurium tends to give polymeric tridimensional networks rather than to dimerize, for instance, as it is often the case with sulfur and selenium. The result is that more tellurium-containing phases than

0022-4596/92 $5.00

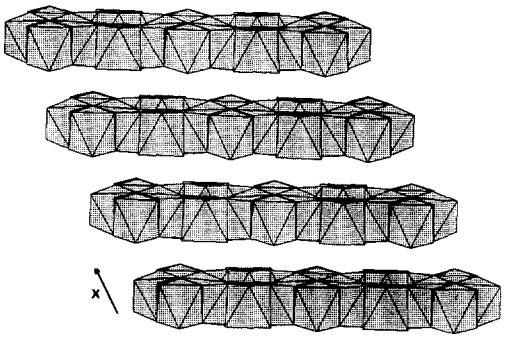

FIG. 1. Perspective drawing of $Cr_{2/3}Te_2$ showing the layered feature of the phase. Between ($Te–Cr_{2/3}\square_{1/3}–Te$) planes no Te–Te bond exists.

expected have a polymeric nature. To prove this, it is necessary not only to observe carefully the Te···Te distances (a length of about 3.55 Å seems to be already a bonding one), but also to calculate, whenever possible, the electronic overlap population between the anions. Such tellurium links decrease the charge borne by the anions, i.e., the oxidation state of tellurium, which may frequently become fractional (between -1 and -2).

$CrTe_3$ could very well be a candidate for inter-anionic multiple bonds, since, with a very stable $Cr^{3+}(d^3)$, one has a mean low oxidation state for tellurium. Also, with a reported layered structure, a metallic behavior could lead to electronic instability in relation with the particular Fermi surface expected in such a case. All these reasons have led to the study presented in this article. After a brief recall of the structure of this phase, the Te···Te distances are carefully examined to detect weak bonding possibilities. Extended Hückel calculations are given and possible bonding interactions between anions are discussed.

II. $CrTe_3$ Structure Description

$CrTe_3$ exhibits a layered structure (Fig. 1) whose sheets consist of building groups of four edge-linked $CrTe_6$ octahedra (shaded regions in Fig. 2) which are connected to four other neighboring groups through apical tellurium atoms to give a two-dimensional infinite arrangement. In addition, these groups are also linked together via Te–Te bonds (see broken and continuous lines linking tellurium atoms in clear surfaces in Fig. 2), giving rise to the formation of Te_2 and Te_3 entities. As shown by Klepp and Ipser (*1*), the very stable Cr^{3+} expected in the phase imposes a mean oxidation state of -1 on the tellurium anions, which is achieved according to the formulation $[Cr^{3+}]_2[Te^{2-}][Te_2]^{2-}[Te_3]^{2-}$ as deduced from the interatomic distances. This phase is thus a true anionic mixed valence compound, and this illustrates once more the original and versatile response of the tellurium anions to a given cationic oxidation state, since one could have had a phase with a polymeric tellurium as in $IrTe_2$ ($Ir_n^{3+}(Te^{-1.5})_{2n}$) (here $Cr_n^{3+}(Te^{-1})_{3n}$). Within the polyanions, the interatomic distances are equal to 2.816 and 2.824 Å for Te_3 and 2.817 Å for Te_2. Although somewhat longer than in the regular pyrite $Mn^{2+}(Te_2)^{2-}$ com-

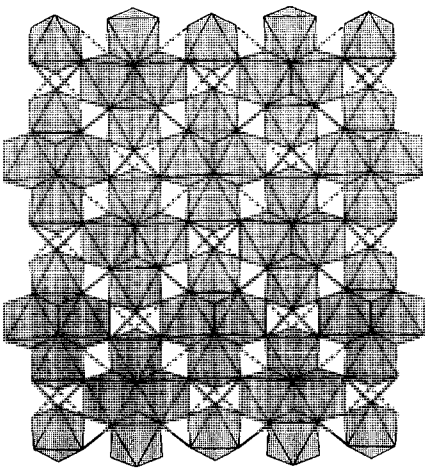

FIG. 2. Projection, in the (*bc*) plane, of the structure of $Cr_{2/3}Te_2$. The phase is built from four edge-sharing octahedra linked through apical tellurium and Te–Te and Te–Te–Te groups.

TABLE I

STRUCTURAL PARAMETERS OF $CrTe_3$ (*1*). MAIN INTERATOMIC DISTANCES (IN Å) AND Te–Cr–Te ANGLES (IN °)

Crystalline system: monoclinic

Lattice parameters:

$a = 7.887(6)$ Å, $b = 11.22(2)$ Å, $c = 11.56(1)$ Å, $\beta = 118.41(2)°$, $Z = 8$, $V = 899.8$ Å^3

Space group: $P2_1/c$

$x \quad y \quad z \qquad -x \quad y + \frac{1}{2} \quad -z + \frac{1}{2}$

$-x \quad -y \quad -z \qquad x \quad -y + \frac{1}{2} \quad z + \frac{1}{2}$

Positional parameters

Te_1	0.2316(5)	0.9078(3)	0.5744(3)
Te_2	0.2722(4)	0.3258(3)	0.2444(3)
Te_3	0.2722(4)	0.1698(3)	0.4354(3)
Te_4	0.2063(5)	0.6196(3)	0.4003(3)
Te_5	0.3005(5)	0.4458(3)	0.5973(3)
Te_6	0.2026(5)	0.6193(3)	0.7325(3)
Cr_1	0.0010(10)	0.0009(8)	0.6691(7)
Cr_2	0.0210(10)	0.2753(8)	0.5075(7)

Principal bond distances of $CrTe_6$ octahedra

Cr_1–Te_1	2.725	Cr_2–Te_1	2.700
Cr_1–Te_1	2.737	Cr_2–Te_2	2.747
Cr_1–Te_2	2.709	Cr_2–Te_3	2.755
Cr_1–Te_3	2.701	Cr_2–Te_4	2.749
Cr_1–Te_4	2.734	Cr_2–Te_5	2.724
Cr_1–Te_6	2.716	Cr_2–Te_6	2.748
Te_1–Te_1	3.822[a]	Te_2–Te_1	4.035[a]
Te_2–Te_1	3.507	Te_3–Te_1	4.016[a]
Te_2–Te_1	4.035[a]	Te_3–Te_2	3.572
Te_3–Te_1	3.437	Te_4–Te_1	3.764
Te_3–Te_1	4.016[a]	Te_4–Te_2	4.048[a]
Te_4–Te_1	3.878	Te_5–Te_2	3.548
Te_4–Te_2	3.908	Te_5–Te_3	3.570
Te_4–Te_3	3.960[a]	Te_5–Te_4	4.077[a]
Te_6–Te_1	3.861	Te_6–Te_1	3.777
Te_6–Te_2	3.927[a]	Te_6–Te_3	4.059[a]
Te_6–Te_3	3.886	Te_6–Te_4	3.854
Te_6–Te_4	3.903[a]	Te_6–Te_5	4.052[a]

Angles Te–Cr–Te around the metal atoms

Te_1–Cr_1–Te_1	88.81	Te_1–Cr_2–Te_2	95.58
Te_1–Cr_1–Te_2	80.16	Te_1–Cr_2–Te_3	94.81
Te_1–Cr_1–Te_3	95.22	Te_1–Cr_2–Te_4	87.35
Te_1–Cr_1–Te_4	90.29	Te_1–Cr_2–Te_6	87.79
Te_1–Cr_1–Te_2	95.89	Te_2–Cr_2–Te_3	80.96
Te_1–Cr_1–Te_3	78.63	Te_2–Cr_2–Te_4	94.86
Te_1–Cr_1–Te_6	90.41	Te_2–Cr_2–Te_5	80.85
Te_2–Cr_1–Te_4	91.78	Te_3–Cr_2–Te_5	81.31
Te_2–Cr_1–Te_6	92.76	Te_3–Cr_2–Te_6	95.04
Te_3–Cr_1–Te_4	93.55	Te_4–Cr_2–Te_5	96.30
Te_3–Cr_1–Te_6	91.68	Te_4–Cr_2–Te_6	89.04
Te_4–Cr_1–Te_6	91.47	Te_5–Cr_2–Te_6	95.55
Te_1–Cr_1–Te_6	172.76	Te_1–Cr_2–Te_5	175.07
Te_1–Cr_1–Te_4	172.01	Te_2–Cr_2–Te_6	174.96
Te_2–Cr_1–Te_3	172.97	Te_3–Cr_2–Te_4	175.45

Shortest interlayer Te–Te distances (in Å)

Te_1–Te_2	4.333
Te_1–Te_3	4.063
Te_1–Te_5	3.857
Te_2–Te_4	4.253
Te_2–Te_5	3.925
Te_2–Te_6	4.069
Te_3–Te_4	4.321
Te_3–Te_6	4.132
Te_4–Te_5	3.945

Te–Te distance in the Te_2 pair (in Å)

Te_2–Te_3	2.817
(Te_4–Te_6)[b]	3.506

Te–Te distances in the Te_3 polyanions (in Å)

Te_4–Te_5	2.816
Te_5–Te_6	2.824

[a] Tellurium in the same sandwich and on each side of this one.

[b] Te–Te distance perpendicular to the pair Te_2 and belonging to the same sandwich in two parallel anionic planes of the layer.

pound (2.750 Å) (*5*), these values fall in the expected range for rather normal Te–Te bonds. It is to be pointed out that in the very ionic phases K_2Te_3 and Rb_2Te_3, the $(Te_3)^{2-}$ groups present distances between 2.796 and 2.805 Å, which are somewhat smaller, whereas more electropositive cesium gives a still shorter bond length of 2.770 Å (*6*, *7*). This tendency may be related to the charge change on the Te_3 and Te_2 groups, and may indicate in the case of $CrTe_3$ the occurrence of lower actual charges than indicated by the formal ones. In Table I are reported some important Cr–Te and Te–Te distances calculated from the data of Ref. (*1*). An examination of these distances shows the following features: (i) On each side of the van der Waals gap the distances between closest tellurium atoms reveal no bonds since they range from 3.857 Å for the shortest to 3.946 Å for the longest (they are 4.02 Å in $HfTe_2$ and $ZrTe_2$) (*8*); the compound is thus a true layered phase. (ii) Within the sheets,

Te(1), Te(2), Te(3), and possibly Te(5) are engaged in Te···Te contacts (see Table I) close enough to allow incipient bonding within the 2D planes. If all these close contacts involve bonding interactions, this would lead to the occurrence of some type of polymeric network within the 2D layers. (iii) The mean Cr–Te distance of 2.728 Å allows one to calculate, with an effective radius for Te^{2-} ions of 2.10 Å, a chromium radius of 0.63 Å, which compares well with that of 0.62 Å of Shannon (*9*) in chalcogenides for Cr^{3+} in an octahedral environment (a value of 0.68 Å is found in layered and structurally related 2D $CrSiTe_3$ for the same ion) (*10*).

Clearly the structural data back up a single cation–anion charge balance. However, because of the unusual character of tellurium among chalcogenides and the occurrence of short Te···Te contacts within the layers, it is not clear what the transport properties of $CrTe_3$ should be. In view of the current interest on the electronic properties of chromium tellurides (*11, 12*), we decided to carry out conductivity and magnetic measurements as well as electronic structure calculations on $CrTe_3$.

III. Conductivity and Magnetic Properties of $CrTe_3$

The phase bulk prepared according to (*1*) showed systematically the presence of magnetic impurities. This came not exactly as a surprise, since the Cr–Te system contains many compounds not all well defined with many nonstoichiometric regions. However, susceptibility measurements made between 300 and 450 K yielded a linear variation of the reciprocal susceptibility with a calculated moment of $\mu = 3.63$ B.M., in agreement with a Cr^{3+} cation. Repeated grindings of the samples followed by annealing at temperatures lower than that of the synthesis ($T = 420$°C) allowed us to obtain preparations in which impurities could not be detected by X-ray analysis, although their presence was still felt on the magnetic data. We did not achieve the synthesis of a completely pure bulk, and we could not obtain enough crystallites to grind for use as powders for the measurements. However, the relative purity of the compound was thought sufficient to give meaningful conductivity data with regard to the present study.

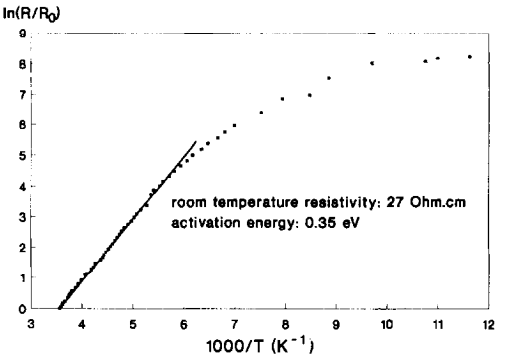

FIG. 3. Electrical properties of $CrTe_3$ showing the semiconducting behavior of the phase, with an activation energy of 0.35 eV.

The conductivity measurements performed from 300 to 80 K on pressed bars with four silver contacts showed a variation versus temperature of the semiconducting type (Fig. 3). From this curve, an activation energy of 0.35 eV can be obtained. The room temperature resistivity is equal to 27 Ohm cm. The observed activation energy may correspond either to the semiconductor true gap or to an electronic interaction energy between cationic sites (Hubbard) (*13*).

IV. Electronic Structure of $CrTe_3$

In order to gain some insight into the electronic structure of $CrTe_3$, we carried out calculations for its 3D network as well as for several of its structural building blocks. Both the tight-binding and molecular calculations used an Extended Hückel-type Ham-

TABLE II

PARAMETERS AND EXPONENTS USED IN THE CALCULATIONS

Atom	Orbital	H_{ii} (eV)	ζ_1	ζ_2	c_1^a	c_2^a
Te (*15*)	5s	−20.78	2.510			
	5p	−13.20	2.160			
Cr (*16*)	4s	−8.66	1.70			
	4p	−5.24	1.70			
	3d	−11.20	4.95	1.80	0.5058	0.6747

[a] Contraction coefficients used in the double-ζ expansion.

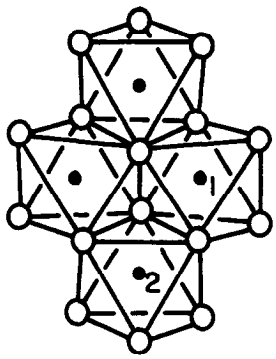

SCHEME I

iltonian (*14*) with the atomic parameters and exponents summarized in Table II. The t_{2g}-block band structure of $CrTe_3$ along the a^*, b^*, and c^* directions is reported in Fig. 4. According to the formal oxidation states of $(Te)^{2-}$, $(Te_2)^{2-}$, and $(Te_3)^{2-}$, there are 24 electrons per repeat unit (Cr_8Te_{24}) to be distributed among the t_{2g}-block levels of $CrTe_3$. The calculated Fermi level assuming double occupancy of the levels is shown as a dotted line in Fig. 4. Three features of Fig. 4 are worthy of comment. First, the band dispersion along the interslab direction

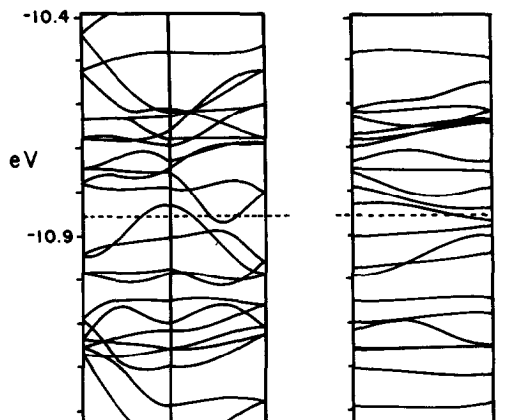

FIG. 4. Dispersion relations for the t_{2g}-block bands of $CrTe_3$ where Γ, X, Y, and Z refer to the wavevectors (0,0,0), (a^*/2,0,0), (0,b^*/2,0), and (0,0,c^*/2), respectively. The dotted line refers to the calculated Fermi level assuming double occupancy of the levels.

($\Gamma \rightarrow X$) is extremely small. This confirms the structural analysis of Section II, i.e., $CrTe_3$ is a real layered material. Second, even for the interslab directions ($\Gamma \rightarrow Y$ and $\Gamma \rightarrow Z$) the t_{2g}-block bands are quite flat, the maximum dispersion being of the order of 0.2 eV. Calculations for other lines of the Brillouin zone show that this is a general result. Third, there is no band gap at the Fermi level. With the two last observations in mind it is clear that $CrTe_3$ is not a regular semiconductor (i.e., one that has no partially filled bands in a one-electron band picture) but a Mott–Hubbard one (i.e., a semiconductor despite the presence of partially filled bands in a one-electron band picture).

It is important to understand the structural origin of this feature. As discussed in Section II, the $CrTe_3$ slabs can be considered to originate from condensation of (Cr_4Te_{16}) clusters (Scheme 1). Every cluster shares half of the tellurium atoms with other clusters in the slab (i.e., $CrTe_3$ can be written as $Cr_4Te_8Te_{8/2}$). In the process of this condensation, very short Te–Te contacts (i.e., true bonds) are created. Thus in order to understand the transport properties of $CrTe_3$ we should consider the nature of the interactions between t_{2g} orbitals within and between the (Cr_4Te_{16}) units. Shown in Fig. 5 are the t_{2g}-block levels for a series of building blocks of the $CrTe_3$ slab. Those of the

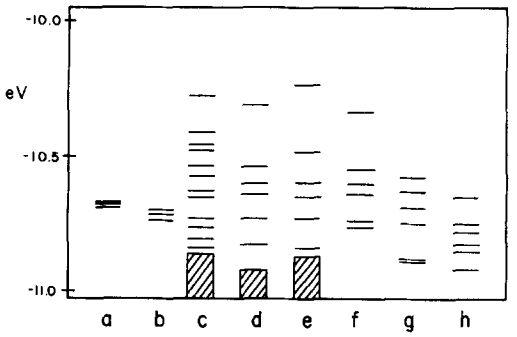

FIG. 5. t_{2g}-block orbitals for different structural building blocks of $CrTe_3$: (a) $Cr(1)Te_6$, (b) $Cr(2)Te_6$, (c) Cr_4Te_{16}, (d) Cr_2Te_{10} (Cr(1)–Cr(2) = 3.67 Å), (e) Cr_2Te_{10} (Cr(1)–Cr(2) = 3.64 Å), (f) Cr_2Te_{10} (Cr(1)–Cr(1) = 3.90 Å), (g) Cr_2Te_{11}, and (h) Cr_2Te_{12}. The dashed blocks in (c), (d), and (e) represent the top of the Te p-block.

two different types of octahedra found in $CrTe_3$ ($Cr(1)Te_6$ and $Cr(2)Te_6$) are reported in Figs. 5(a) and (b), respectively. The two sets of t_{2g} orbitals have a very weak splitting and are found at very similar energies. This is a consequence of the quite similar and regular nature of these octahedra. The t_{2g}-block levels of the (Cr_4Te_{16}) cluster are reported in Fig. 5(c). There is no net separation between the top of Te p-block (shaded in Fig. 5c) and the bottom of the Cr t_{2g}-block. In fact, there is a quite sizeable mixing of these Te and Cr orbitals in the region around -11.0 eV. Because of this fact, the location of the top of the t_{2g}-block with respect to the levels of the isolated octahedra is a better measure of the strength of the interaction than the total width of the t_{2g}-block. The top of the t_{2g}-block levels in the cluster coincides with the top of the t_{2g}-block bands in the $CrTe_3$ slab. Thus the essential orbital interactions in the $CrTe_3$ slab should be already present in the (Cr_4Te_{16}) cluster. Every cluster contains two types of ($CrTe_6$) octahedra ($Cr(1)Te_6$ and $Cr(2)Te_6$, see Scheme 1) and three different types of (Cr_2Te_{10}) edge-shared octahedra: $Cr(1)Cr(2)Te_{10}$ (Cr(1)–Cr(2) = 3.67 Å), $Cr(1)Cr(2)Te_{10}$ (Cr(1)–Cr(2) = 3.64 Å), and

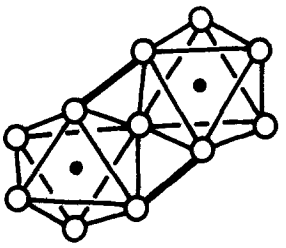

SCHEME 2

$Cr(1)Cr(1)Te_{10}$ (Cr(1)–Cr(1) = 3.90 Å). The t_{2g}-block levels of the three (Cr_2Te_{10}) clusters are reported in Figs. 5(d), (e), and (f), respectively. The top of the three t_{2g}-block levels are very similar, the slight differences reflecting the differences in Cr–Cr distances. This means that the three different types of interaction within the (Cr_4Te_{16}) cluster are of comparable strength. On the basis of these results we can conclude that there are moderate but non-negligible interactions within the (Cr_4Te_{16}) units. The metal levels of the $CrTe_3$ slab result mainly from Cr(2)–Cr(1) interactions via corner sharing of two octahedra (see Scheme 2) or through Cr(2)–Cr(2) interactions via Te–Te bonded octahedra (see Scheme 3). These interactions can be modelled by performing calculations on the (Cr_2Te_{11}) and (Cr_2Te_{12}) clusters shown in schemes 2 and 3, respectively. In contrast with the results for the (Cr_2Te_{10})

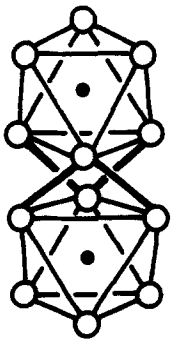

SCHEME 3

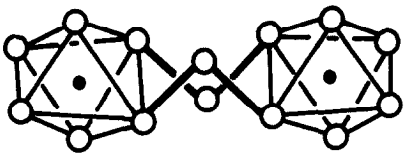

SCHEME 4

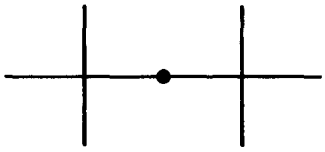

SCHEME 6

clusters, the top of the t_{2g}-block (see Figure 5(g) and (h)) lies in both cases very near the levels of the isolated octahedra indicating very weak interactions. This is easy to understand for the (Cr_2Te_{12}) clusters because only metal–metal through-bond-type interactions via the $(Te_3)^{2-}$ units could lead to some coupling. In this case, however, the geometry of the condensation does not favor any orbital interaction of this type. Let us note that the same argument applies for the possible Cr(1)–Cr(1) interaction through $(Te_3)^{2-}$ units represented in Scheme 4. The (Cr_2Te_{11}) cluster contains two corner-shared octahedra (see Schemes 2 and 5). When the *M–X–M* angle is ≈180° (see Scheme 6), two of the t_{2g} orbitals of each octahedra interact strongly through the *X p*-type orbitals. However, when the corner sharing is as shown in Scheme 5, the coupling between t_{2g} orbitals, either direct through space, indirect through overlap with the orbitals of the shared Te atom, or through-bond via the Te–Te bonds is quite poor and leads to very weak interaction. In consequence, there is almost no communication between the t_{2g} orbitals of the (Cr_4Te_{16}) cluster units in the $CrTe_3$ slabs. This is the reason for the weak band dispersions in Fig. 4.

Another important question to address in the case of $CrTe_3$ is the possibility of incipient polymerization within the tellurium sublattice (*17*). As we have recently shown (*2–4*), the diffuse nature of the Te orbitals can lead to bonding interactions for quite long Te···Te distances. These types of interactions can have an important role in determining the structural or even the transport properties of transition metal tellurides (*2–4, 15, 17, 18*). The easiest way to prove the existence of these additional bonding interactions is by analyzing the corresponding overlap populations (OP). In the present case it is not immediately obvious how to perform such an analysis because of the uncertainty in the occupation of the energy levels. In order to tackle this problem, we decided to calculate these OP for a large number of electron occupations with the hope that some general trends would emerge. We considered all Te···Te pairs with interaction distances smaller than 3.7 Å. The calculated OP were remarkably similar for most of the electron occupations reasonable for $CrTe_3$. We note the following results from our calculations. First, the OP for the three types of Te–Te bonds within the Te_2 and Te_3 groups have very similar values (around 0.5). Second, one of the non-bonded Te···Te interactions, i.e., Te(4)···Te(6) (3.506 Å), has a positive and definitely non-negligible OP (0.02). Third, all other close Te···Te distances have OP suggesting practically no interaction. For instance, the Te(3)···Te(2) (3.572 Å) and Te(2)···Te(1) (3.507 Å) ones are always practically nil or even slightly negative; the Te(2)···Te(5) (3.548 Å), Te(3)···Te(5)

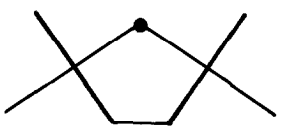

SCHEME 5

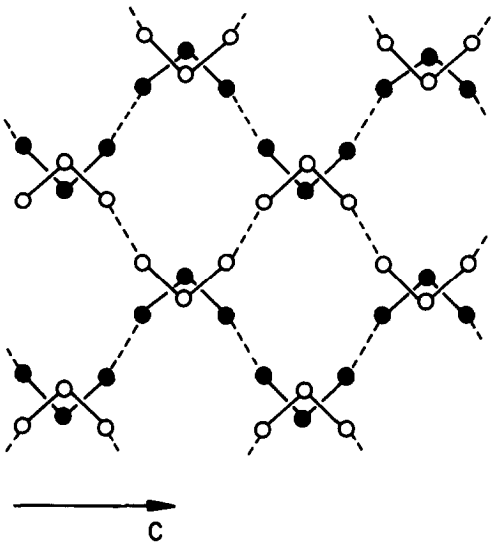

SCHEME 7

(3.570 Å) and Te(3)···Te(1) (3.437 Å) ones are about three times smaller than the Te(4)···Te(6) one. These observations lead to two important conclusions. First, the distance is not necessarily a good criterium to identify bonding interactions. This is particularly clear when comparing the OP for Te(4)···Te(6) (3.506 Å) and Te(3)···Te(1) (3.437 Å). The overlap populations take into account both the distance and directionality of the orbitals implicated in the interaction so that provide a more sensitive criterium. Second, there are definitely non-negligible bonding interactions between the Te(4)···Te(6) atoms. Since this contact provides a connection between two adjacent $(Te_3)^{2-}$ units in the same plane of the layer we can conclude that the $CrTe_3$ slabs contain incipient tellurium zig-zag chains (see Scheme 7) running parallel to the *c* direction of the crystal. In contrast, the Te_2 pairs remain essentially isolated within the tellurium sublattice. Thus $CrTe_3$ provides a further example of a transition metal telluride with a polymerized tellurium sublattice.

V. Dimensionality and Polymerization in Tellurides

The chemistry of tellurides is, for a large part, driven by the particular behavior of tellurium which, with its particular size and redox properties, in relation with its band level positions respective to the metal *d* orbital ones, leads to many varied anionic groupings. Until recently, the difference between true two-dimensional and two-dimensional derived polymerized phases was not really made. Also, the occurrence of extrabonding within three-dimensional arrangements like the pyrite-type phases introduces polymerization as an extra structural factor within already 3D phases. These new observations lead us to distinguish between dimensionality and polymerization, in order to classify the transition metal ditellurides, and beyond them, all the other tellurium-containing phases. Table III shows a classification taking into account the phase dimensionality (2D and 3D) and, within each domain, the degree of polymerization, i.e., the number of directions and ways that tellurium uses to create polymeric networks (from 0 to 4, i.e., along *a*, *b*, and *c* within the slab or through the gap, this being symbolized by *a*, *b*, *c*, G). The degree of polymerization may maintain 2D structures when tellurium bondings take place within the slabs. Bonding through the van der Waals gap gives polymeric 2D-derived compounds and locates the corresponding phases within the three-dimensional domain; 3D compounds undergoing polymerization maintain the phases into the same domain but with a displacement along the diagram axes. Going through the different ditellurides known and classifiable to date (among them $CrTe_3$ considered as $Cr_{2/3}\square_{1/3}Te_2$), one can make the following comments:

A. In the Two-Dimensional Domain

1. True 2D phases are represented by $TiTe_2$, $ZrTe_2$, and $HfTe_2$. $TiTe_2$ seems to be

TABLE III

CLASSIFICATION OF TRANSITION METAL DITELLURIDES TAKING INTO ACCOUNT THE PHASE DIMENSIONALITY (2D AND 3D) AND THE DEGREE OF POLYMERIZATION

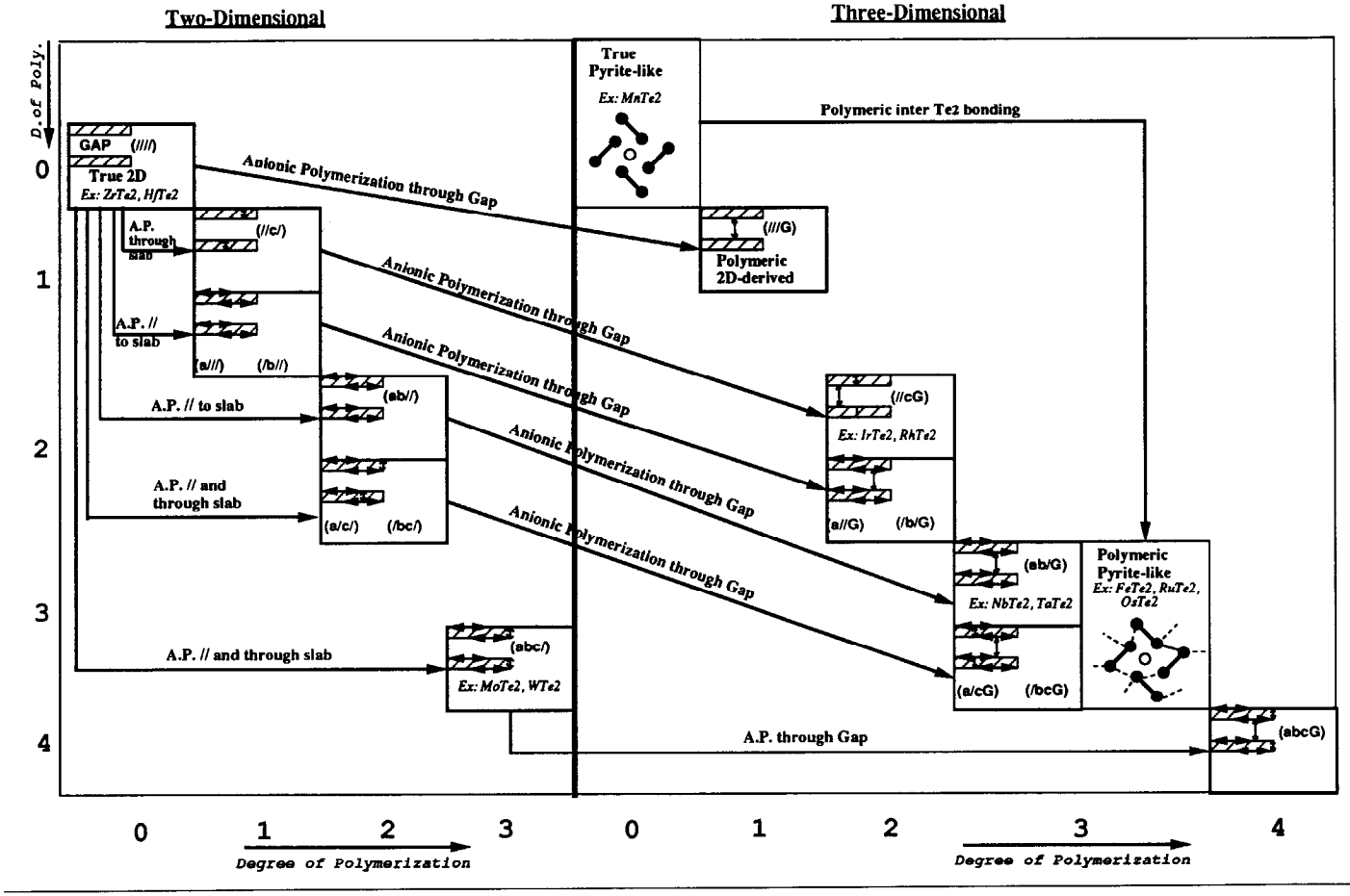

Note. The term "Anionic Polymerization" (A.P.), considered here to classify the structures, corresponds to weak intertellurium bonding taking place in the whole structure. To broadly characterize the direction of those links, two possibilities have been considered: along *a* and/or *b* (in-plane bonding), along *c* (label c for intraslab or G for through gap interslab bonding). In the absence of polymeric bonding, a slash is mentioned in the structure symbol. Those boxes with nothing listed have, to date, no real example.

a border case with a short intraslab Te···Te distance of 3.74 Å (*8*).

2. Within the in-layer polymeric 2D phases domain (left lower part of Table III), through and within-layer bondings seem to be the case for WTe_2 and $MoTe_2$ (*19*) (distances of 3.679 and 3.520 Å, on one hand, and 3.652, 3.671, and 3.493 Å on the other hand, are given for within and through-layer tellurium distances, respectively, for WTe_2 and $MoTe_2$). Of course, as explained before, actual bondings should be proved by physical experiments and calculation. Within and parallel to layer, ID polymerization is to be found in $Cr_{2/3}Te_2$.

B. In the Three-Dimensional Domain

3. True pyrite-like phases ($MnTe_2$ for instance) (zero degree of polymerization) give rise to polymeric pyrite-like phases exemplified by $FeTe_2$, $NiTe_2$, $RuTe_2$, etc., as shown elsewhere (*3, 4*).

4. 3D polymeric 2D-derived phases like $IrTe_2$, $RhTe_2$, $CoTe_{1.7}$, etc., obtained from two-dimensional models present two degrees of polymerization (through-layer and through-gap) (see (*2, 4*)).

5. 3D polymeric 2D-derived compounds with also two degrees of polymerization (parallel to layer and through-gap) can be found. This family can probably be represented by $NbTe_2$ and $TaTe_2$ (*20*) with Te···Te distances parallel to layers of 3.560 and 3.558 Å for $NbTe_2$ and $TaTe_2$ and through-layer lengths of 3.527, 3.600 and 3.595, 3.651 Å. Again there is no true evidence, to our knowledge, of bonding in these phases. However, contrary to the case of WTe_2 and $MoTe_2$ mentioned before, we have here an example of short through-gap distances which do not seem to be implied by internal structural strain. In that case one may assume true anionic bonding.

Although not many complex transition metal tellurides are known to date, several layered ternary compounds were recently made and their structures determined in the $MM'Te_5$ family with M = Nb, Ta, and M' = Ni, Pd for instance (*21–23*). It is of interest to note that very short Te···Te distances of 3.196 Å were calculated. In addition, the magnetic moment obtained for $NbNiTe_5$ (μ_{eff} = 1.24 B.M.) implies a complex and unusual charge transfer between the anions and the metal atoms as evidenced from the compound formula: with five tellurium and a maximum of seven positive charges (Nb^{5+} and Ni^{2+}), tellurium anions must have a low and fractional oxidation state (*24*) and, according to previous observations, polymerization is expected. There is no doubt that many tellurides to be synthesized in the future will pose the same and interesting problem of actual charge transfer.

We believe the recognition of these incipient polymerizations of the tellurium sublattice can play a very fundamental role in understanding the chemistry and physics of transition metal tellurides. In this respect, three different situations should be distinguished. The first one occurs when the polymerization is essential to understand the oxidation states. An example of this situation is provided by the $MM'Te_5$ phases mentioned above. The second one occurs when there is polymerization but it does not clearly modify the formal oxidation states. An example is $CrTe_3$, where creation of the weak additional bonds can be considered to arise from weakening of the initial normal bonds in the $(Te_3)^{2-}$ units and not from charge transfer between the different components of the tellurium network ($(Te)^{2-}$, $(Te_2)^{2-}$, and $(Te_3)^{2-}$) or between the chromium and tellurium sublattices. The third situation refers to the absence of polymerization. It is then quite likely (*18*) that some anomalies in the structural or physical properties of transition metal tellurides are simply related to changes from one to another of these situations, i.e., internal charge transfer and/or bond redistribution. For instance, metal–tellurium charge transfer and

bond redistribution was suggested by Whangbo (*25, 26*) to rationalize the appearance of the low-temperature structural modulation in $NbTe_4$. Formally, the change from the average structure to the incommensurately modulated one in $AuTe_2$ can be considered as an example of charge transfer and bond redistribution within the tellurium network, judging from the results recently reported by Haas and co-workers (*27*) and Krutzen and Inglesfield (*28*). Systematic work on the synthesis and electronic structure of transition metal tellurides is likely to be extremely fruitful.

VI. Concluding Remarks

The main results of our study can be summarized as follows. $CrTe_3$ is a real layered material with a semiconducting behavior. Our magnetic susceptibility measurements are consistent with the oxidation state of +3 for chromium. The $CrTe_3$ slabs are built from the condensation of very regular octahedra which generate (Cr_4Te_{16}) units through Te–Te edge-sharing. These units generate the slab through corner-sharing of half of its Te atoms and formation of Te–Te bonds. Our calculations and measurements show that these slabs contain high-spin Cr^{3+} ions with moderate but non-negligible interactions within the (Cr_4Te_{16}) units, but very weak interactions between these units. Consequently, our study indicates that $CrTe_3$ is a Mott–Hubbard semiconductor rather than a regular one. Interestingly, our results for $CrTe_3$ seem to be consistent with those reported by Kolis and co-workers (*29*) concerning the discrete cluster $(Cr_3Te_{24})^{3-}$. This cluster is built from face-sharing condensation of three $(CrTe_6)$ octahedra and contains six $[Te_4]^{2-}$ ligands leading to an oxidation state of Cr^{3+} for the metal atoms. On the basis of magnetic susceptibility measurements Kolis and co-workers concluded (*29*) that this cluster contains high-spin Cr^{3+} ions with reasonably strong antiferromagnetic coupling. Analysis of the overlap populations for the different Te···Te contacts shows that $CrTe_3$ is another transition metal telluride with a polymerized tellurium network. $CrTe_3$ can be classified in a dimensionality–polymerization diagram, suggested to take into account the various degrees of bonding within the tellurium network.

References

1. O. Klepp and H. Ipser, *Angew. Chem. Int. Ed. Engl.* **21,** 911 (1982).
2. S. Jobic, P. Deniard, R. Brec, J. Rouxel, A. Jouanneaux, and A. N. Fitch, *Z. Anorg. Allg. Chem.* **598–599,** 199 (1991).
3. S. Jobic, M. Evain, R. Brec, P. Deniard, A. Jouanneaux, and J. Rouxel, submitted for publication.
4. S. Jobic, R. Brec, and J. Rouxel, submitted for publication.
5. N. Elliott, *J. Am. Chem. Soc.* **59,** 1958 (1937).
6. B. Eisenmann and H. Schäfer, *Angew. Chem. Int. Ed. Engl.* **17,** 684 (1978).
7. P. Böttcher, *J. Less-Common Met.* **70,** 263 (1980).
8. F. Hullinger, "Structural Chemistry of Layer-Type Phases," D. Reidel Dordrecht, Holland/Boston.
9. R. D. Shannon, *Acta Crystallogr. Sect. A: Cryst. Phys. Diffr. Theor. Gen. Crystallogr.* **32,** 751 (1976).
10. G. Ouvrard, E. Sandre, and R. Brec, *J. Solid State Chem.* **73,** 27 (1988).
11. J. Dijkstra, H. H. Weitering, C. F. van Bruggen, C. Haas, and R. A. de Groot, *J. Phys.: Condens. Matter* **1,** 9141 (1989).
12. J. Dijkstra, C. F. van Bruggen, C. Haas and R. A. de Groot, *J. Phys.: Condens. Matter* **1,** 9163 (1989).
13. (a) N. F. Mott, "Metal Insulator Transitions," Barnes and Noble, New York, 1977; (b) B. H. Brandow, *Adv. Phys.* **26,** 651 (1977).
14. (a) R. Hoffmann, *J. Chem. Phys.* **39,** 1397 (1963); (b) M.-H. Whangbo and R. Hoffmann, *J. Am. Chem. Soc.* **100,** 6093 (1978); A modified Wolfsberg-Helmholz formula was used to calculate the off-diagonal Hij values. See J. H. Ammeter, H.-B. Bürgi, J. Thibeault, and R. Hoffmann, *J. Am. Chem. Soc.* **100,** 3686 (1978).
15. E. Canadell, F. Mathey, and M.-H. Whangbo, *J. Am. Chem. Soc.* **110,** 104 (1988).
16. R. H. Summerville and R. Hoffmann, *J. Am. Chem. Soc.* **98,** 7240 (1976).

17. Incipient polymerization refers to the existence of the Te···Te contacts shorter than the van der Waals distances and associated with positive overlap populations. For a detailed analysis of its strong control of the structural and transport properties of the CdI_2-type transition metal ditellurides, see E. CANADELL, S. JOBIC, R. BREC, J. ROUXEL, AND M. H. WHANGBO, submitted for publication.
18. M. H. WHANGBO AND E. CANADELL, unpublished results.
19. B. E. BROWN, *Acta Crystallogr.* **20,** 268 (1966).
20. B. E. BROWN, *Acta Crystallogr.* **20,** 264 (1966).
21. E. W. LIIMATTA AND J. A. IBERS, *J. Solid State Chem.* **71,** 384 (1987).
22. E. W. LIIMATTA AND J. A. IBERS, *J. Solid State Chem.* **77,** 141 (1988).
23. E. W. LIIMATTA AND J. A. IBERS, *J. Solid State Chem.* **78,** 7 (1989).
24. J. F. HALET, R. HOFFMANN, W. TREMEL, E. W. LIIMATTA, AND J. A. IBERS, *Chem. Mater.* **1,** 451 (1989).
25. M. H. WHANGBO, private communication.
26. A. MEERSCHAUT, J. ROUXEL, *in* "Crystal Chemistry and Properties of Materials with Quasi-One-Dimensional Structures" (J. Rouxel, Ed.), Reidel, Dordrecht (1986).
27. A. VAN TRIEST, W. FOLKERTS, AND C. HAAS, *J. Phys.: Condens. Matter* **2,** 8733 (1990).
28. B. C. H. KRUTZEN AND J. E. INGLESFIELD, *J. Phys.: Condens. Matter* **2,** 4829 (1990).
29. W. A. FLOMER, S. C. O'NEAL, W. T. PENNINGTON, D. JETER, A. W. CORDES, AND J. W. KOLIS, *Angew. Chem. Int. Ed. Engl.* **27,** 1702 (1988).